Electrical pulse triggered reversible assembly of molecular adlayers

Shern-Long Lee,*[a] Yu-Ju Hsu,[a] Hung-Jen Wu,[a] Hsing-An Lin,[b] Hsiu-Fu Hsu,*[b] and Chun-hsien Chen*[a]

[a] Department of Chemistry and Centre for Emerging Material and Advanced Devices, National Taiwan University, Taipei, Taiwan, 10617
[b] Department of Chemistry, Tamkang University, Tamsui, Taiwan 25137

Experimental details

Literature procedures[S1] were followed to prepare hexakis((3,4-bis(dodecyloxy)-phenyl)ethynyl)benzene, **1**. All chemicals were ACS grade or better and were TCI, including tetrabutylammonium perchlorate and solvents of 1-phenyloctane, 1,2,4-trichlorobenzene, octane, *n*-tetradecane.

STM imaging was carried out in constant current mode, at room temperature and the liquid-solid interface by a PicoScan (Agilent Technologies). HOPG (highly orientated pyrolytic graphite) was from Advanced Ceramics (ZYH grade). The STM probes were commercially available Pt/Ir tips (PT, Nanotips, Veeco Metrology Group/Digital Instruments, USA). Imaging parameters of E_{bias} and $i_{tunnelling}$ ranged, respectively, from 0.10 to 1.50 V and from 10 to 400 pA. The lattice structures of **1** reported in this *Communication* were calibrated by the corresponding unit cell vector of the underlying HOPG. The structures were examined by several tips and samples to avoid artefacts. The limitations of the applied voltage were ±10 V. The electrical pulses were applied by a built-in program (Fig. S1) of PicoScan. Note that the tip performance, in terms of imaging resolution at the molecular level, might become unrecoverable for $E_{pulse} > 7$ V, which are thus not recommended. After the application of E_{pulse} within 3~6 V, about 20% of the tips showed deteriorated performance and required another pulses to get recovered. It is important to select E_{pulse} in a reasonable range, for example, from 3 V to 6 V, which has been employed in literature.[S2,S3] The images and molecular models were prepared by WSxM 5.0 and Gaussian03, respectively.

References

S1. S.-L. Lee, H.-A. Lin, Y.-H. Lin, H.-H. Chen, C.-T. Liao, T.-L. Lin, Y.-C. Chu, H.-F. Hsu, C.-h. Chen, J.-J. Lee, W.-Y. Hung, Q.-Y. Liu and C. Wu, *Chem.–Eur. J.*, 2011, **17**, 792.

S2. K. S. Mali, D. Wu, X. Feng, K. Müllen, M. Van der Auweraer and S. De Feyter, *J. Am. Chem. Soc.*, 2011, **133**, 5686.

S3. M. Li, K. Deng, Y.-L. Yang, Q.-D. Zeng, M. He and C. Wang *Phys. Rev. B*, 2007, **76**, 155438.

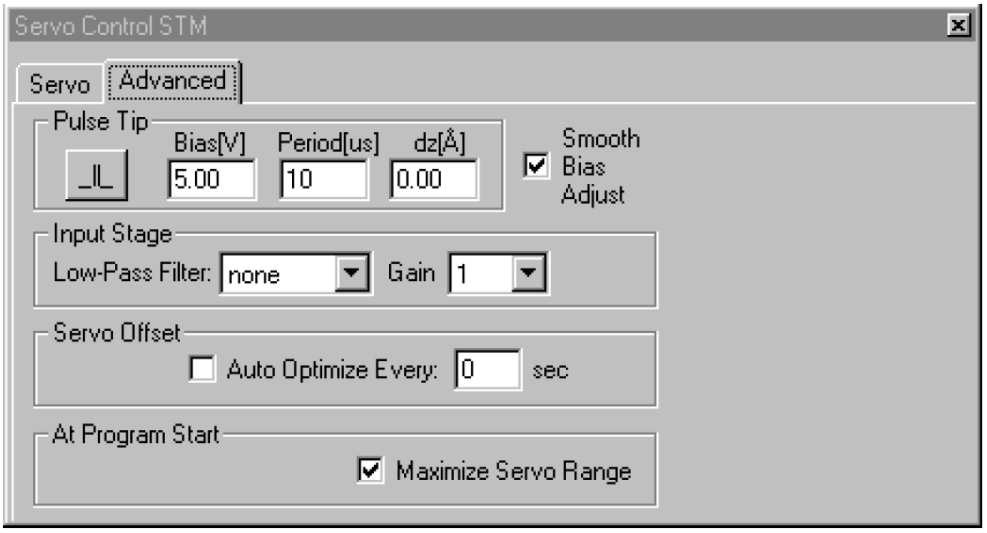

Fig. S1. Dialogue window for the generation of electrical pulses. This function is a built-in program (PicoScan, Agilent Technologies) to trigger the pulse without disrupting the image acquisition. Upon activating this function, the tip is withdrawn the distance of dz (in Å) away from where the tip is imaging, applying a bias with the preset voltage (Bias in Volt) and duration (Period in μs), and subsequently returning to the imaging position. The available range of bias voltages, duration of pulse, and dz are ±10 V, 1–65535 μs, and 0–2 μm, respectively. Typical operating conditions: E_{bias}, 0.8 V; $i_{tunnelling}$, 60 pA; Bias, 3–5 V; Period, 10 μs.

Solvent and concentration dependence for the pulse-triggered assembly.

The following images show that the 5-V/10-μs triggered formation of honeycomb nanopores is quite general. Solvents of phenyloctane (main text), octane, 1,2,4-trichlorobenzene, and *n*-tetradecane (Fig. S2) as well as concentrations of 1 mM and 1 μM (in phenyloctane, Fig. S3) all confer the nanoporous structure. Panels a1 and a2 of Fig. S2 were obtained in air (*i.e.*, the solid-gas interface) prior to and after the application of a 5-V/10-μs pulse, respectively. In contrast, for examples shown in Panels b~d of Fig. S2, the honeycomb nanopores were formed by delivering a pulse in media containing 1-μM **1**. The difference suggests that the formation of nanopore structure involves deposition of molecules in the solvent onto the monolayer.

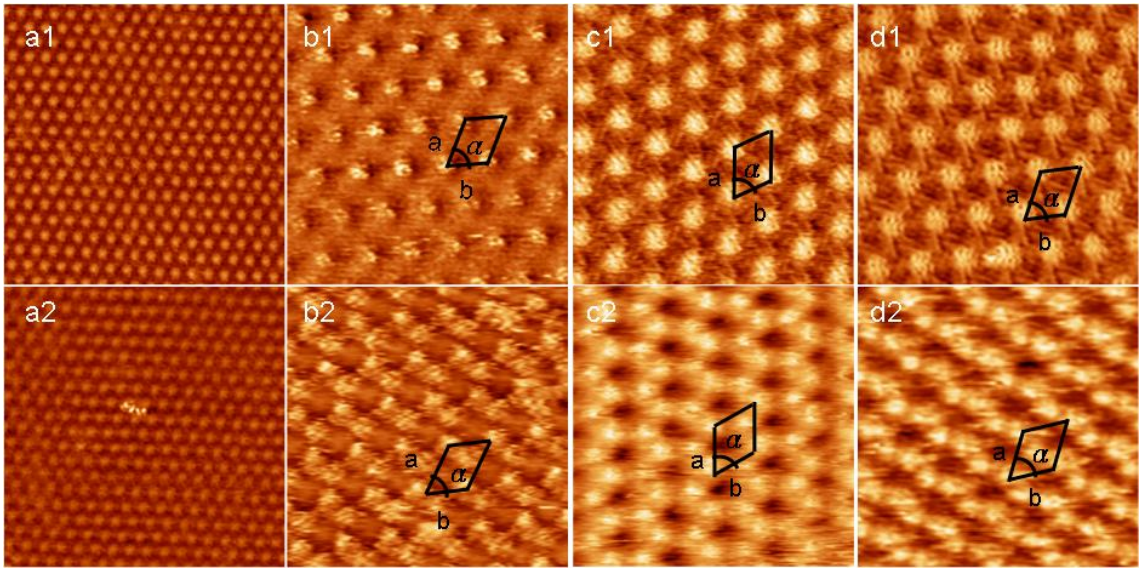

Fig. S2. Images of **1** (upper) prior to and (lower) after the application of an electrical pulse of 5 V/10 μs (a) in air and in solvents of (b) octane, (c) 1,2,4-trichlorobenzene, and (d) *n*-tetradecane. For Panels a, the sample was prepared in octane (without rinsing). After the evaporation of octane, the pulse was applied to the gas/solid interface yet the formation of nanopores did not take place. For Panels b, the experiments were carried out in a liquid cell to avoid octane evaporation. The difference between Panels a2 and b2 confirms the proposed mechanism that the electrical pulse deposits molecules from solution down to the surface. The pulse-induced patterning appears general in all solvents used.. Unit cell parameters of $|\vec{a}|$, $|\vec{b}|$, and α: (b1) 3.5 (± 0.2) nm, 3.4 (± 0.2) nm, 62° (± 3°); (b2) 3.4 (± 0.3) nm, 3.3 (± 0.2) nm, 61° (± 2°); (c1) 3.4 (± 0.2) nm, 3.4 (± 0.2) nm, 60° (± 2°); (c2) 3.3 (± 0.3) nm, 3.6 (± 0.3) nm, 63° (± 3°); (d1) 3.4 (± 0.3) nm, 3.4 (± 0.3) nm, 59° (± 3°); (d2) 3.4 (± 0.3) nm, 3.1 (± 0.2) nm, 58° (± 3°). Conditions: solutions, 1-μM **1** in the corresponding solvent; image size: a: 50 x 50 nm, b-d: 20 x 20 nm; E_{bias}, $i_{tunnelling}$: (a) 0.7 V, 50 pA; (b) 0.8 V, 36 pA; (c) 0.8 V, 350 pA; (d) 0.8 V, 80 pA.

The effect of applying a 5-V/10-μs pulse has been examined in phenyloctane containing 1-mM, 1-μM, and 1-nM **1** (Fig. S3a~c). The formation of nanopores takes place for the former two concentrations. Under the low concentration of 1 nM, the resulted structure appeared incomplete nanopores. The section profiles shown in Fig. S4 reveal that the pulse-deposited molecules bear a higher apparent height than those of the neighbouring **1** in the monolayer. Presented in Panel d1 and d2 of Fig. S3 are images obtained in 1-nM **1** before and a few imaging frames after the monolayer being treated by a 4-V/10-μs pulse. Panel d2 shows that adsorbed molecules were found on top of the underlying aromatic cores (white arrows) and moved afterwards (solid green arrows).

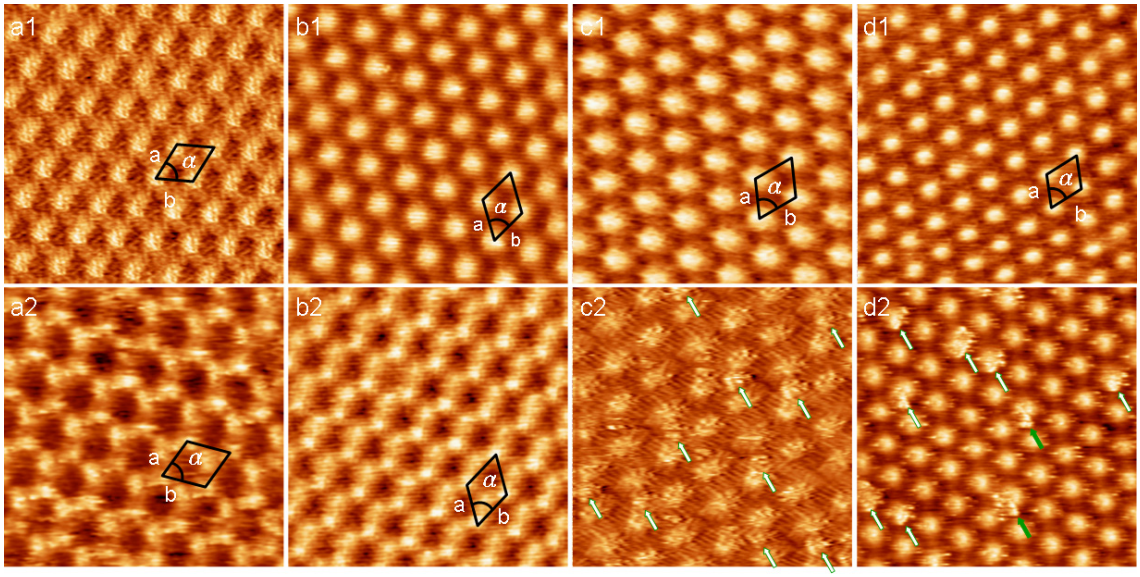

Fig. S3. STM images (upper) prior to and (lower row) after the application of (a~c) a 5-V/10-μs pulse and (d) a 4-V/10-μs pulse in phenyloctane containing **1** of (a) 1 mM, (b) 1 μM, and (c,d) 1 nM. Panels c2 and d2 demonstrate that the attempt of using a low concentration of **1** (nanomolar-level) led to unsuccessful formation of nanoporous and bilayer patterns, ascribed to an insufficient amount of molecules in solution. The arrows highlight the incompletely deposited **1** on the alkoxy chains of the first layer of **1**. Unit cell parameters of $|\vec{a}|$, $|\vec{b}|$, and α: (a1) 3.3 (± 0.2) nm, 3.3 (± 0.2) nm, 60° (± 2°); (a2) 3.4 (± 0.3) nm, 3.4 (± 0.2) nm, 60° (± 3°); (b1) 3.4 (± 0.2) nm, 3.5 (± 0.2) nm, 62° (± 2°); (b2) 3.4 (± 0.2) nm, 3.3 (± 0.3) nm, 63° (± 3°); (c1,d1) 3.4 (± 0.2) nm, 3.4 (± 0.2) nm, 60° (± 2°). Imaging conditions: E_{bias}, 0.8 V; $i_{tunnelling}$, 60 pA. Image size: (a) 24 x 24 nm, (b) 23 x 23 nm, (c) 21 x 21 nm, (d) 27 x 27 nm.

Justification of the proposed structures: concerns of imaging artefacts

A concern that has been carefully looked into is the possibility of pulse-induced tip-reshaping, particularly the double-tip effects, leading to the images presented in Fig. 1 in the main text. Although the structural transformation synchronises consistently with the electrical pulses (*e.g.*, Fig. 2 in the main text), we have managed to acquire Fig. S4~S9 to negate the scenario that the proposed structures of bilayers and nanopores are misinterpreted from imaging artefacts. In Fig. S4, obtained in 1-nM **1**, the section profiles across the incomplete nanopore and the underlying first layer allows us to assign the higher protrusion to molecules of the electrically deposited second layer. The section profile provided in Fig. 5 further supports the presence of two apparent heights. In Fig. S7a, the defects indicated by the arrows clarify that the image is not a result of the double-tip effects which would exhibit overlapped tunnelling currents and are not able to show random defects. The defect sites in fact expose the underlying molecules. Noticeably, the brightest positions of the overlayer and underlying molecules (at the defect sites) both appear off-centred yet shifted toward opposite directions. The brightest points for those at the adlayer are located at the left to the centre and those at the defects are at the right, suggesting the molecules at the top layer being slipped slightly from the underlying ones, leading to the proposed bilayer structure (see Fig. 1b in the main text). Fig. S7b shows structures of the hexagonal monolayer and the nanopores, separated by a domain boundary going vertically across the image frame. The presence of two structures along the horizontal direction of the image manifests that the reported structures are not associated with the tip shapes. Molecular features at the domain boundary appear relatively fuzzy, indicative of dynamic adsorption-desorption of **1**. Note that it was not easy to find defects and that the domain boundary was located at the periphery of the applied pulse.

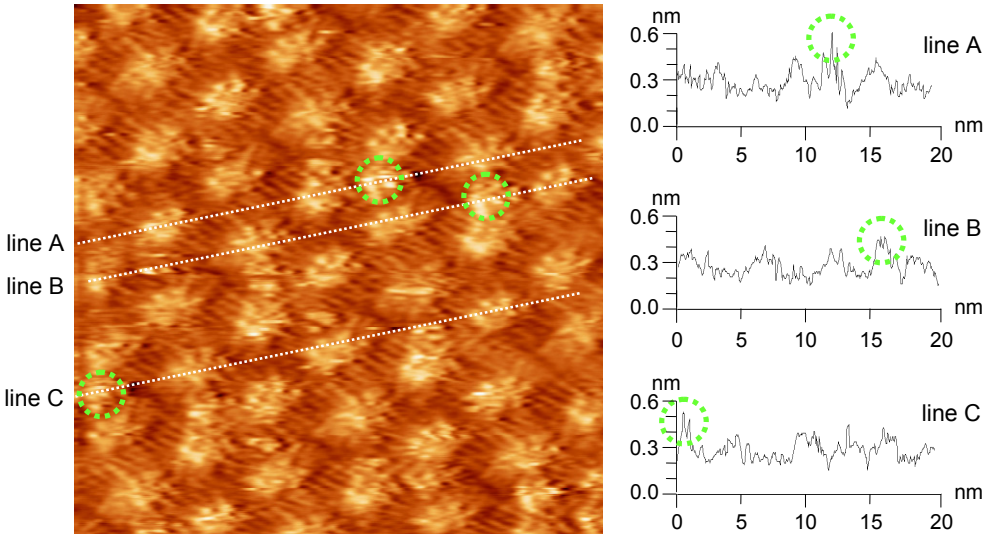

Fig. S4. Section profiles of incomplete nanoporous structure. This image is Panel c2 of Fig. S3. The section profiles show that pulse-deposited **1** exhibits a higher apparent height than the neighbouring molecules.

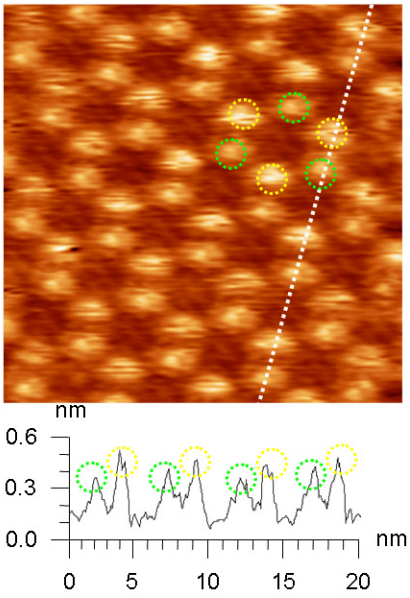

Fig. S5. Section profile of the nanoporous structure. The section profile and the image contrast throughout the manuscript indicate two sets of molecular positions. The yellow circles denote the higher set of **1** sitting on alkyl chains of the lower set (green circles). Specifically, based on the section profiles revealed in Fig S4, molecules of the lower set are attributed to those adsorbed on HOPG prior to the electrical pulse and most of their alkyl chains are in contact with the substrate. After the electrical pulse, the aromatic cores of **1** in the second layer sit on the alkyl chains of those in the first layer. The details are described in the main text (page 2, right column, lines 60-68). Experimental conditions: the same as those of Fig. S3b2. Image size: 20 x 20 nm.

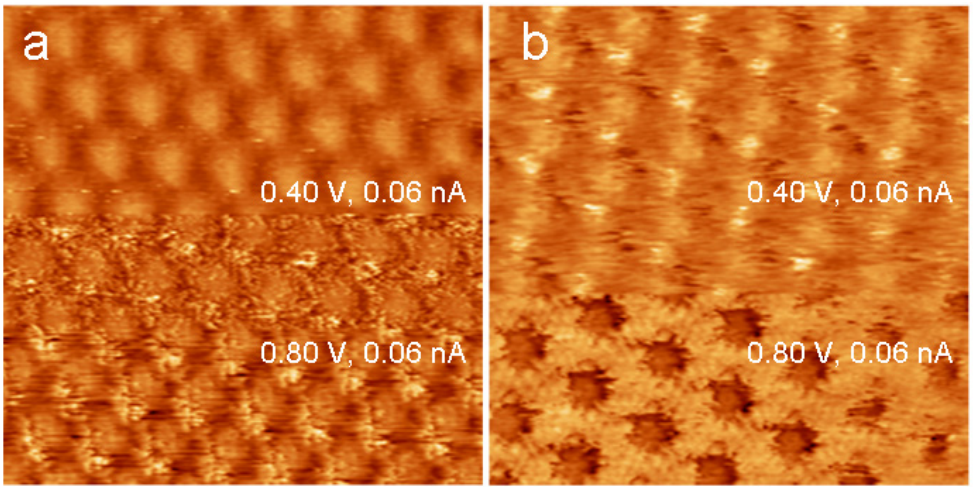

Fig. S6. STM images unravelling underlying structures of (a) bilayer and (b) nanopore by smaller imaging impedance. The purpose of this attempt is to assess the structural correlation of the adlayers to the underlying ones. Images of (a) bilayer and (b) honeycomb assemblies were prepared by applying pulses of 4 V and 5 V, respectively. The scan directions for both frames were from the bottom going upward. Scanning into the middle of the frames, a smaller E_{bias} and thus tunnelling impedance was employed to have the tip approaching closer to the underlying layer. The upper portions of the images indicate that the underlayers are hexagonal monolayers, similar to those prepared by 3-V pulses. To be cautious, the experiments have been examined repeatedly and the results are reproducible. Although the images appear hazy, it always shows the characteristics of hexagonal monolayers under conditions of small imaging impedance. The result suggests that both structures are composed of an adlattice on top of the hexagonal monolayer. Image size: 22 x 22 nm. Solutions: 1-μM **1** in phenyloctane.

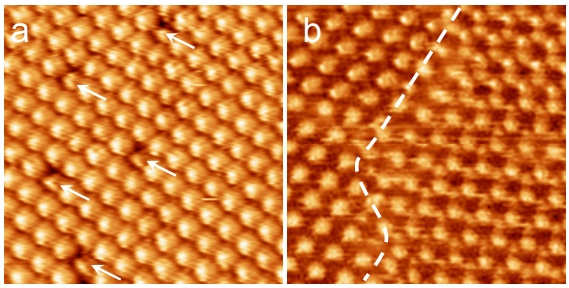

Fig. S7. STM images of (a) point defects and (b) a domain boundary. The features exclude false structural assignment due to pulse-induced re-shaping of the STM tip. The random defects and the presence of both structures of the hexagonal monolayer and the nanopores justify the data acquisition and the structural assignment. Image size: 30 x 30 nm. Other conditions are the same as those in Fig. 1 in the main text.

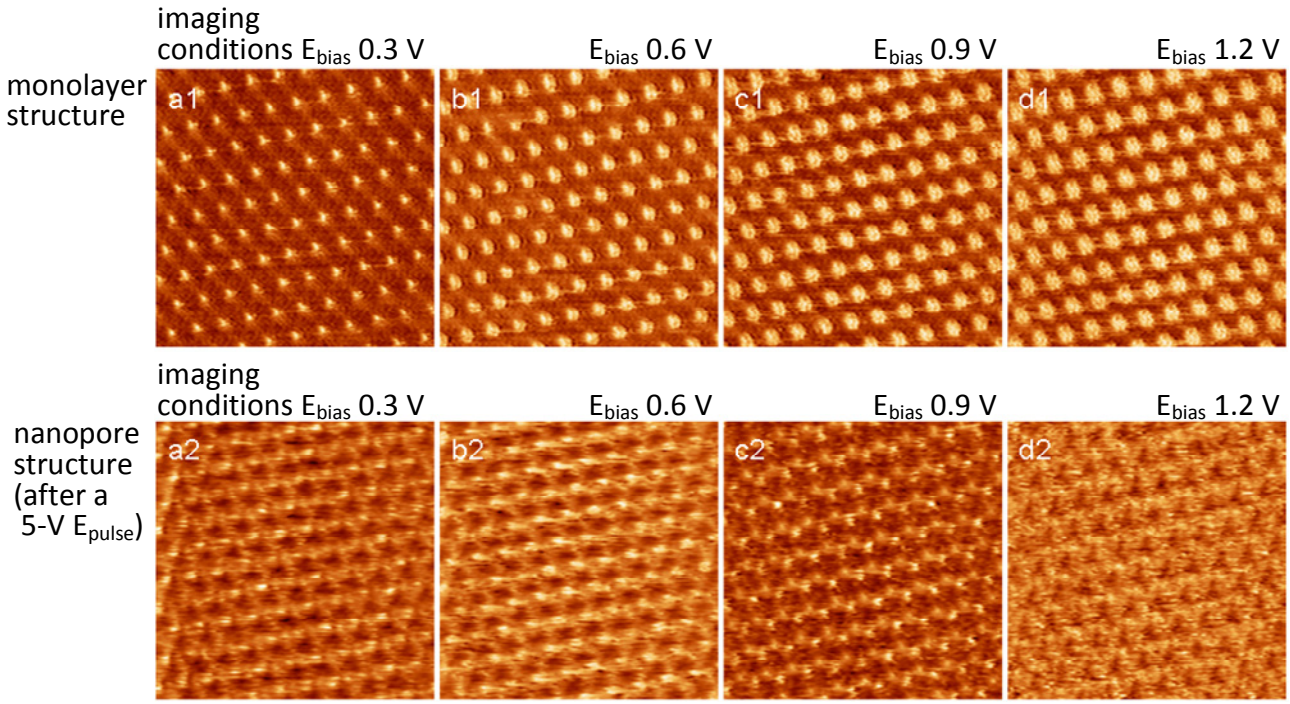

Fig. S8. The effect of imaging bias on the observed structures of (upper row) hexagonal monolayers and (lower) honeycomb nanopores. The concerns of imaging conditions which probe electronic clouds at different orbitals and result in hexagons and nanopores are also examined. The images were acquired at imaging bias of (a) 0.3 V, (b) 0.6 V, (c) 0.9 V, (d) 1.2 V, (upper) prior to and (lower) after the monolayer was subjected to an electrical pulse of 5 V/10 μs. The images in the upper row exhibit the same hexagonal structure and so do those in the lower row with honeycomb features. Since the arrangement of **1** appears independent of imaging bias, E_{bias}, the applied electrical pulse is the dominant driving force for the structural transformation. Although Panels a2 and b2 are ill-defined, they both show the honeycomb features with an additional molecule sits between the apparent ones. Note that the imaging conditions were not optimised and the STM tip might be in contact with the films. Conditions: $i_{tunnelling}$, 30 pA; frame size, 30 nm x 30 nm. The solution contained 1.0-μM **1** in phenyloctane.

The Effect of the strength of the electric field on the domain size of nanopores

As what stated in the main text, in this study the field strength of the electrical pulse has been studied by adjusting the tip-substrate distance and by introducing electrolytes. The instrument allows us to reposition the tip without interrupting the scanning and the assessment of the imaging location (see Fig. S1). Therefore, how the domain size is affected by the tip-substrate distance can be scrutinised. In the following, dz is defined as the retracted distance of the tip from the imaging position determined by E_{bias} and $i_{tunnelling}$. Fig. S9a was obtained after exerting to a hexagonal monolayer a 5-V pulse at a dz 500-nm above its imaging position. The adlattice structure appears unaffected by the electrical stimulus. With a smaller dz of 20 nm, Fig. S9b and c show an approximate 50-nm ring of the honeycomb structure encircled by the surrounding hexagonal monolayer. The domain size is about 250 nm for a further smaller dz of 1~5 nm. At dz = 0 nm (*i.e.*, under the same imaging conditions as those of Fig. 1 in the main text with E_{bias} = 0.8 V and $i_{tunnelling}$ = 60 pA), the domain size is larger than the 500-nm imaging range that the STM scanner can perform. The dependence of domain size on dz and the assembly taking place proximal to the tip support the hypothesis that the electrical field emitted via the tip enables the deposition of molecules. This is also supported by the performance associated with tip sharpness. The use of blunt tips makes the formation of stimuli-induced adlattices not as reproducible as that of the sharp ones. In addition, the domain size is found shrunk with a higher concentration of electrolytes (Fig. S10). Under the same imaging conditions as those of Fig. 1 in the main text, the domain sizes of the honeycomb nanopores are reduced to 150 nm and 60 nm in solutions containing 1-μM and 0.1-mM tetrabutylammonium percholorate, respectively. The presence of charged electrolytes shields the electrical field and leads to a smaller degree of molecular polarisation. The electrolytes also develop a potential drop between the tip and substrate, diminishing the surface area which is able to afford an effective local charge strong enough to attract the polarised molecules onto the substrate.

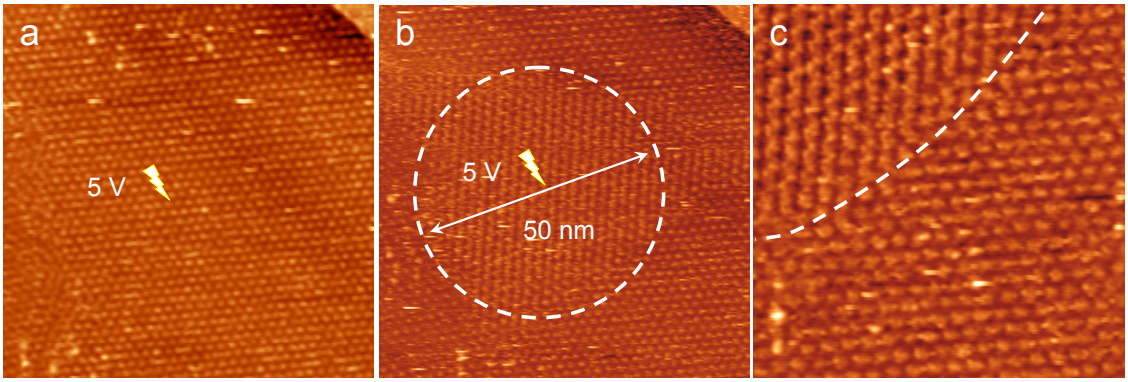

Fig. S9. The effect of the field strength of the electrical pulse on the domain size of honeycomb nanopores. The STM images were obtained, without aborting the image acquisition, after a 5-V/10 μs pulse applied at the tip being retracted (a) 500 nm and (b,c) 20 nm from the imaging position. Prior to the pulses, the imaging was operated under conditions of 0.8-V E_{bias} and 60-pA $i_{tunnelling}$. After the pulse was delivered, the tip immediately returned to the imaging position. The step edge at the upper right corner of Panels a and b was deliberately recorded to pinpoint the identical location for the two images. Panel c is a magnified image of Panel b and shows the domain boundary between the honeycomb (upper left) and the hexagonal lattices. The diameter of the pulse-triggered domain in (b) is roughly 50 nm. The imaging conditions of 0.8-V E_{bias} and 60-pA $i_{tunnelling}$ were employed to obtain all the images. Frame size: (a) 85 nm x 85 nm, (b) 85 nm x 85 nm, (c) 36 nm x 36 nm.

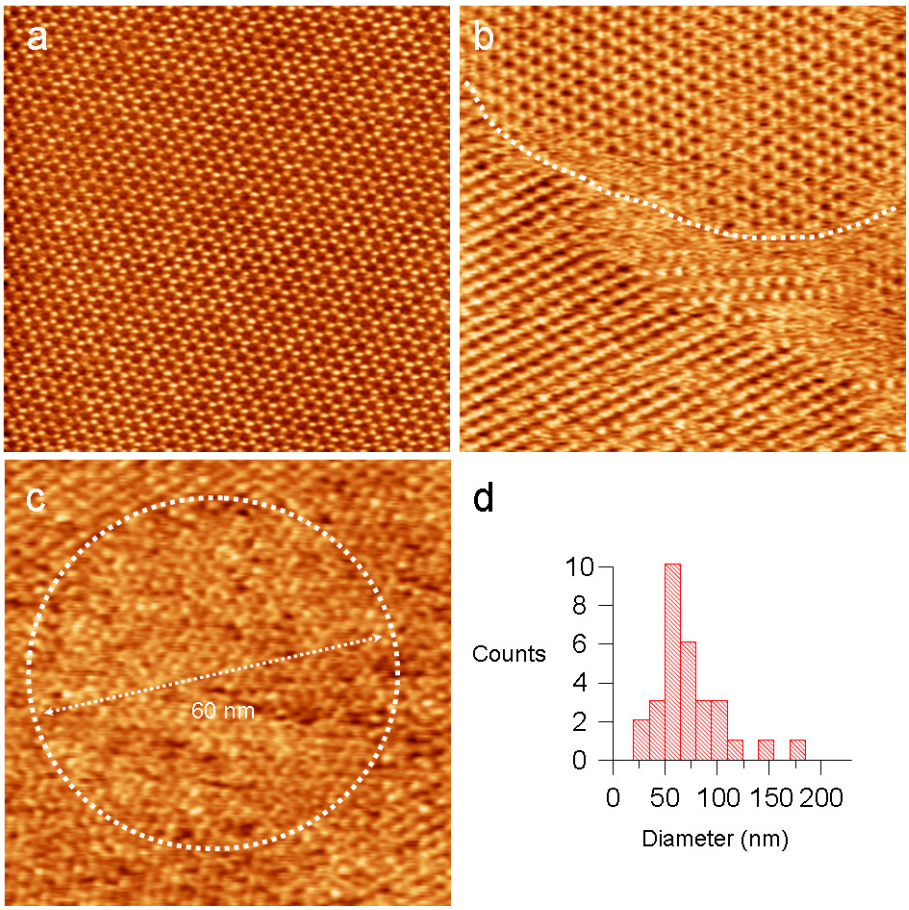

Fig. S10. The effect of electrolytes on the domain size of honeycomb nanopores. The images were acquired after an electrical stimulus of 5 V/10 μs. Concentrations of tetrabutylammonium percholorate (TBAP): (a) 0 μM; (b) 1 μM; (c) 100 μM. Panel (d) is a histogram of the nominal diameters of the honeycomb domains collected from 30 runs under the conditions of Panel c. The curvatures of the white dashed lines in Panels b and c are used to estimate the domain size. The image quality of Panel c is somewhat obscure, attributed to the current leakage and the interference due to the presence of high-concentration TBAP. Conditions: solutions, 1-μM **1** in phenyloctane; E_{bias}, 0.8 V; $i_{tunnelling}$, 60 pA. Image size: 75 x 75 nm. The bin size for Panel d is 15 nm.